LETTERS
PUBLISHED ONLINE: 25 JULY 2016 | DOI: 10.1038/NPHYS3837
nature physics

Contribution of quasar-driven outflows to the extragalactic gamma-ray background

Xiawei Wang* and Abraham Loeb

The origin of the extragalactic γ-ray background permeating throughout the Universe remains a mystery forty years after its discovery[1]. The extrapolated population of blazars can account for only half of the background radiation in the energy range of ∼0.1–10 GeV (refs 2,3). Here we show that quasar-driven outflows generate relativistic protons that produce the missing component of the extragalactic γ-ray background and naturally match its spectral fingerprint, with a generic break above ∼1 GeV. The associated γ-ray sources are too faint to be detected individually, explaining why they had not been identified so far. However, future radio observations may image their shock fronts directly. Our best fit to the Fermi-LAT observations of the extragalactic γ-ray background spectrum provides constraints on the outflow parameters that agree with observations of these outflows[4–7] and theoretical predictions[8,9]. Although our model explains the data, there might be additional contributing sources.

The components of the extragalactic γ-ray background (EGB) have been a puzzle since its discovery four decades ago[10]. Recently, the Large Area Telescope (LAT) on Fermi provided a fifty-month measurement of the integrated emission from γ-ray sources, with photon energies extending from 0.1 to 820 GeV (ref. 2). The latest analysis of Fermi-LAT data implies that both resolved and unresolved blazars account for $\sim 50^{+12}_{-11}\%$ of the EGB in the energy range of 0.1–10 GeV, leaving the origin of the remaining component in question[3].

Active galactic nuclei (AGN) are observed to exhibit strong outflows, with velocities of $\sim 0.1c$, as manifested by broad absorption lines[5,7]. The ratio between the input kinetic luminosity of the outflows $L_{\rm in}$ and the bolometric luminosity of quasars $L_{\rm bol}$, $f_{\rm kin}$, is observationally inferred to be $f_{\rm kin} \sim 1$–5% (refs 4–7). The shock wave produced by the interaction of a quasar-driven outflow with the surrounding interstellar medium is expected to accelerate protons to relativistic energies, similarly to the shocks surrounding supernova (SN) remnants, where observations of γ-ray emission due to decay of neutral pion (π^0) indicate relativistic proton–proton (pp) collisions via $\rm pp \rightarrow \pi^0 \rightarrow 2\gamma$ (ref. 11). Here, we calculate the analogous γ-ray emission from quasar-driven outflows.

The energy distribution of accelerated protons per unit volume can be written as $N(E_{\rm p}) = N_0 E_{\rm p}^{-\Gamma_{\rm p}}$, where $E_{\rm p}$ is the proton energy, N_0 is a normalization constant, and the power-law index $\Gamma_{\rm p} \sim 2$–3, based on theoretical models[12] and observations of shocks around SN remnants[11,13]. We adopt a fiducial value of $\Gamma_{\rm p} \sim 2.7$ and show that our results are not very sensitive to variations around this value (see Supplementary Fig. 1 for details). N_0 can be constrained by the total energy condition $\epsilon_{\rm nt} E_{\rm th} = \int_{E_{\rm min}}^{E_{\rm max}} N(E_{\rm p}) E_{\rm p}\, {\rm d}E_{\rm p}$, where $E_{\rm th}$ is the thermal energy density of the shocked particles and $\epsilon_{\rm nt} \sim 10\%$ is the fraction of the shock kinetic energy converted to accelerate protons[14]. The minimum energy of the accelerated protons, $E_{\rm min}$, is set to be the order of the proton rest energy $m_{\rm p}c^2$ and their maximum energy, $E_{\rm max}$, is obtained by equating the acceleration time of protons, $t_{\rm acc}$, to either the timescale of pp collision, $t_{\rm pp} \sim (n_{\rm p}\sigma_{\rm pp}c)^{-1} \approx 10^8 n_{\rm p,0}\sigma_{\rm pp,-26}$ yr, or the dynamical timescale of the outflow shock $t_{\rm dyn} \sim R_{\rm s}/v_{\rm s} \approx 10^6 R_{\rm s,kpc} v_{\rm s,3}^{-1}$ yr. For typical values of the outflow parameters, $E_{\rm max}$ is of the order of 10^6 GeV. The e-folding time to accelerate protons to relativistic energies is $t_{\rm acc} \sim E_{\rm p}c/eBv_{\rm s}^2 \approx 300 E_{\rm p,TeV} B_{-6}^{-1} v_{\rm s,3}^{-2}$ yr, where $E_{\rm p,TeV} = (E_{\rm p}/{\rm TeV})$, e is the electron charge and $B = 10^6 B_{-6}$ G is the magnetic field strength[15]. We assume a fraction of the post shock thermal energy, $\xi_{\rm B}$, is carried by the magnetic field and adopt $\xi_{\rm B} \sim 0.1$, in analogy with SN remnants[16], and we have verified that our results are not sensitive to variations around this value. Here, $n_{\rm p,0} = (n_{\rm p}/1\,{\rm cm}^{-3})$ is the proton number density, $\sigma_{\rm pp,-26} = (\sigma_{\rm pp}/10^{-26}\,{\rm cm}^2)$ is the inelastic cross section of pp collision, and $R_{\rm s,kpc} = (R_{\rm s}/1\,{\rm kpc})$ and $v_{\rm s,3} = (v_{\rm s}/10^3\,{\rm km\,s}^{-1})$ are the radius and velocity of the outflowing shell, which can be obtained by solving the hydrodynamics of the outflows[17] (see Methods for details).

The contribution from quasar outflows to the EGB can be estimated by summing the γ-ray emission over the known quasar population of all bolometric luminosity at all redshifts. The cumulative specific intensity is given by:

$$I(E_\gamma) = \iint \Phi(L_{\rm bol}, z) \frac{\bar{L}_\gamma(E'_\gamma, L_{\rm bol}, z)}{4\pi D_{\rm L}^2(z)} \exp[-\tau_{\gamma\gamma}(E'_\gamma, z)] \times \frac{{\rm d}V}{{\rm d}z\,{\rm d}\Omega}\, {\rm d}\log L_{\rm bol}\, {\rm d}z \quad (1)$$

where $E'_\gamma = E_\gamma(1+z)$ is the intrinsic photon energy, $\Phi(L_{\rm bol}, z)$ is the quasar bolometric luminosity function[18] and $D_{\rm L}(z)$ is the luminosity distance to redshift z. $\bar{L}_\gamma(E_\gamma, L_{\rm bol}, z) = t_{\rm Sal}^{-1} \int L_\gamma(E_\gamma, \tau, L_{\rm bol}, z)\, {\rm d}\tau$ is the time-averaged γ-ray luminosity of an individual quasar outflow, where $t_{\rm Sal} \sim 4 \times 10^7$ yr is the Salpeter time for a radiative efficiency of 10% (ref. 19; see Methods for details). The diffuse extragalactic background light (EBL) associated with the cumulative ultraviolet–optical–infrared emission by star-forming galaxies and AGN over the wavelength range of 0.1–10^3 μm, attenuates high-energy photons via e^+e^- pair production. The high-energy γ-ray spectrum is therefore attenuated by photon–photon scattering on the EBL, through a factor of $\exp(-\tau_{\gamma\gamma})$, where $\tau_{\gamma\gamma}(E_\gamma, z)$ is the EBL optical depth[20] for photons with energy E_γ at a redshift of z.

Figure 1 shows the cumulative γ-ray emission from quasar-driven outflows. We set upper and lower limits on the contribution from radio galaxies to the EGB on the basis of the most recent Fermi-LAT catalogue (3FGL)[21] and find that radio galaxies can account for $\sim 7 \pm 4\%$ of the EGB at $E_\gamma \lesssim 10$ GeV, roughly two to five times less than previous estimates based on sources identified in the first and second Fermi-LAT catalogue (1FGL[22] and 2FGL[23]). Insufficient knowledge of the γ-ray emission's origin and core variability of radio galaxies lead to uncertainties in the estimation of their contribution

Department of Astronomy, Harvard University, 60 Garden Street, Cambridge, Massachusetts 02138, USA. *e-mail: xiawei.wang@cfa.harvard.edu

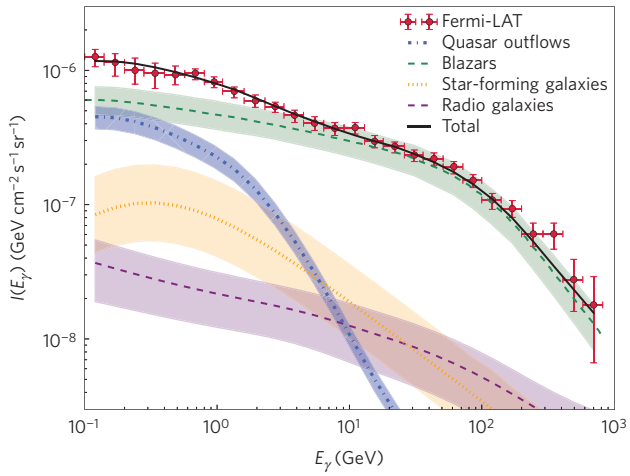

Figure 1 | Spectral energy distribution of the integrated γ-ray background. Fermi-LAT data of the extragalactic γ-ray background is shown as the red points with error bars taken from Ackermann and colleagues[2]. The green dashed line corresponds to the contribution from blazars as estimated by Ajello and colleagues[3]. The purple dashed line shows the contribution from radio galaxies, following Inoue[22] and Di Mauro *et al.*[23], derived from the most recent sample in the Fermi-LAT catalogue[21] (Ackermann *et al.* 2015). The orange dotted line corresponds to the contribution from star-forming galaxies as estimated by Ackermann *et al.*[24], assuming the γ-ray emission spectral shape follows that of the MW. The dot-dashed blue line represents the contribution from our quasar-driven outflow model with $\eta_{-3}=3.98$, where $\eta_{-3}=(\eta/10^{-3})$. The total contribution to EGB from all sources is shown as the solid black line. The shaded regions indicate the uncertainties of each component.

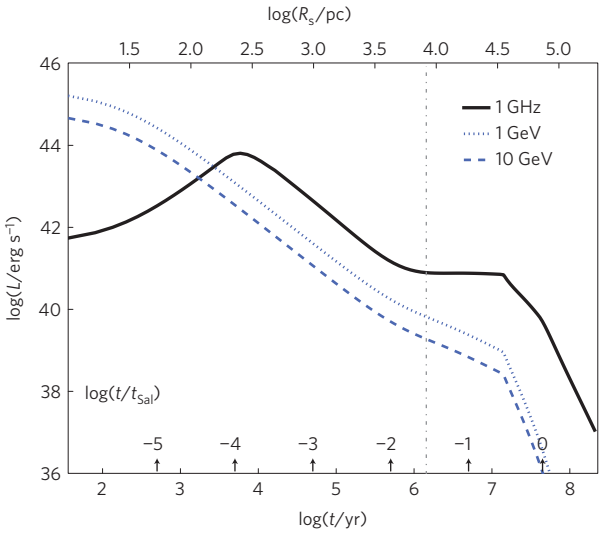

Figure 2 | Light curve of γ-ray emission from AGN-driven outflows and its radio counterpart, for a halo mass $M_{halo}=10^{12}\,M_\odot$ and redshift $z=0.1$. The solid black line represents the radio synchrotron emission at 1 GHz from electrons accelerated at the outflow shock front[17]. The dotted and dashed blue lines show the γ-ray emission from accelerated protons with photon energies at 1 GeV and 10 GeV, respectively. The dot-dashed vertical line marks the transition of the outflow from the disk to the halo of its host galaxy. The radio and γ-ray luminosity are shown as a function of time, t, and outflow shock radius, R_s, on the lower and upper horizontal axes, respectively. Above the lower horizontal axis, we express the time as a fraction of the Salpeter time t_{Sal}, indicating roughly the probability of finding a quasar at each time or position. The vast majority of the quasar outflows are too faint to be detected individually, explaining why their contribution to the EGB had not been recognized.

to the EGB (see Methods for details). Star-forming galaxies have been evaluated to constitute $\sim 13 \pm 9\%$ of the EGB[24]. We show that the contribution from quasar outflows takes up the remaining ∼20–40% of the EGB, which is dominant over the total of radio galaxies and star-forming galaxies, and can naturally account for the amplitude and spectral shape of the remaining EGB, while at higher energies the EGB is dominated by blazars[3]. We have verified that the cumulative contribution from radio galaxies and star-forming galaxies does not match the spectral shape of the EGB, in that the EGB would be overproduced at $E_\gamma \gtrsim 10$ GeV if the sum of radio galaxies and star-forming galaxies makes up the missing component at $E_\gamma \lesssim 10$ GeV. We find that the break in the spectral energy distribution (SED) of quasar outflows at $\lesssim$10 GeV is independent of the parameter choices for the outflow dynamics. This generic cutoff in the emission spectrum of quasar outflows naturally fits the missing EGB component.

The fraction of the shock kinetic energy used to accelerate protons ϵ_{nt} and the fraction of the quasar's bolometric luminosity that powers the outflow f_{kin} are free parameters whose product $\eta=\epsilon_{nt}f_{kin}$ can be constrained by the EGB data. We search for the minimum of $\chi^2=\sum_{i=1}^{N}(I^i_{obs}-I^i_{mod})^2/\Delta_i^2$ throughout the parameter space, where N is the number of data points, Δ_i is the error bar of the ith observed point, and I^i_{obs} and I^i_{mod} are the EBG intensity of the observed and expected values, respectively. We find the best fit value of $\eta=(3.98\pm0.76)\times10^{-3}$ at 90% significance. For $\epsilon_{nt}\sim10\%$, as inferred from observations of SN remnants[11] and theoretical models[12,14], we deduce a value of $f_{kin}\sim$1–5%, which agrees well with observations of outflows[5–7] and theoretical predictions[8,9].

The bright phase of the γ-ray emission from an individual quasar ends abruptly when the outflow exits from the surrounding galactic disk, as shown in Fig. 2, making it difficult to detect afterwards. Outflows embedded in Milky Way (MW) mass halos propagating to 10-kpc scale are expected to produce GeV γ-ray emission of $\sim10^{39}$–10^{40} erg s^{-1}. In the local Universe ($z<0.1$), we find that only $\lesssim$0.1% of quasars host γ-ray bright outflows that are detectable by Fermi-LAT at GeV energies. These outflows are too faint to be detected in γ-rays individually, explaining why they have not been identified so far. A possible candidate for a galactic outflow relic is the Fermi bubbles at the Galactic centre[25], whose γ-ray emission has been explained by a hadronic process similar to our model[26,27]. Our interpretation can be tested through observations of quasar outflows at other wavelengths. Radio emission is simultaneously produced via synchrotron radiation from accelerated electrons by the same outflow shocks (see black solid line in Fig. 2). Radio telescopes such as the Jansky Very Large Array and the Square Kilometre Array provide high sensitivity to detect this emission and confirm the parameters of outflows[17] at redshifts of up to ∼5. For most AGN, the radio emission is free of contamination from the central source or scattering of its light by surrounding electrons. Source stacking[28] could be performed in the future to find direct evidence for the cumulative γ-ray signal from multiple outflow-hosting quasars. The calibration of the outflow parameters based on their γ-ray emission can be used to forecast their contribution to the neutrino background through pion production in pp collisions (X. Wang and A. Loeb, manuscript in preparation).

Methods

Methods, including statements of data availability and any associated accession codes and references, are available in the online version of this paper.

Received 19 October 2015; accepted 22 June 2016; published online 25 July 2016; corrected online 3 August 2016

References

1. Kraushaar, W. L. *et al*. High-energy cosmic gamma-ray observations from the OSO-3 satellite. *Astrophys. J.* **177,** 341–363 (1972).
2. Ackermann, M. *et al*. The spectrum of isotropic diffuse gamma-ray emission between 100 MeV and 820 GeV. *Astrophys. J.* **799,** 86–110 (2015).
3. Ajello, M. *et al*. The origin of the extragalactic gamma-ray background and implications for dark matter annihilation. *Astrophys. J.* **800,** L27–L34 (2015).
4. Fabian, A. C. Observational evidence of active galactic nuclei feedback. *Annu. Rev. Astron. Astrophys.* **50,** 455–489 (2012).
5. Arav, N. *et al*. Quasar outflows and AGN feedback in the extreme UV: HST/COS observations of HE 0238–1904. *Mon. Not. R. Astron. Soc.* **436,** 3286–3305 (2013).
6. Cicone, C. *et al*. Massive molecular outflows and evidence for AGN feedback from CO observations. *Astron. Astrophys.* **562,** 21–46 (2014).
7. Tombesi, F. *et al*. Wind from the black-hole accretion disk driving a molecular outflow in an active galaxy. *Nature* **519,** 436–438 (2015).
8. Zubovas, K. & King, A. Clearing out a galaxy. *Astrophys. J.* **745,** L34–L39 (2012).
9. King, A. & Pounds, K. Powerful outflows and feedback from active galactic nuclei. *Annu. Rev. Astron. Astrophys.* **53,** 115–154 (2015).
10. Fornasa, M. & Sanchez-Conde, M. A. The nature of the diffuse gamma-ray background. *Phys. Rep.* **598,** 1–58 (2015).
11. Ackermann, M. *et al*. Detection of the characteristic pion-decay signature in supernova remnants. *Science* **339,** 807–811 (2013).
12. Caprioli, D. Cosmic-ray acceleration in supernova remnants: non-linear theory revised. *J. Cosmo. Astropart. Phys.* **07,** 38–56 (2012).
13. Ackermann, M. *et al*. Search for early gamma-ray production in supernovae located in a dense circumstellar medium with Fermi LAT. *Astrophys. J.* **807,** 169–184 (2015).
14. Caprioli, D. & Spitkovsky, A. Simulatioms of ion acceleration at non-relativistic shocks. I. Acceleration efficiency. *Astrophys. J.* **783,** 91–108 (2014).
15. Blandford, R. & Eichler, D. Particle acceleration at astrophysical shocks: a theory of cosmic ray origin. *Phys. Rep.* **154,** 1–75 (1987).
16. Chevalier, R. A. Sychrotron self-absorption in radio supernovae. *Astrophys. J.* **499,** 810–819 (1998).
17. Wang, X. & Loeb, A. Probing the gaseous halo of galaxies through non-thermal emission from AGN-driven outflows. *Mon. Not. R. Astron. Soc.* **453,** 837–848 (2015).
18. Hopkins, P. F., Richards, G. T. & Hernquist, L. An observational determination of the bolometric quasar luminosity function. *Astrophys. J.* **654,** 731–753 (2007).
19. Yu, Q. & Tremaine, S. Observational constraints on growth of massive black holes. *Mon. Not. R. Astron. Soc.* **335,** 965–976 (2002).
20. Stecker, F. W., Malkan, M. A. & Scully, S. T. Intergalactic photon spectra from the far-IR to the UV Lyman limit for $0 < z < 6$ and the optical depth of the Universe to high-energy gamma rays. *Astrophys. J.* **658,** 1392 (2007).
21. Ackermann, M. *et al*. The third catalog of active galactic nuclei detected by the Fermi Large Area Telescope. *Astrophys. J.* **810,** 14–48 (2015).
22. Inoue, Y. Contribution of gamma-ray-loud radio galaxies' core emissions to the cosmic MeV and GeV gamma-ray background radiation. *Astrophys. J.* **733,** 66–75 (2011).
23. Di Mauro, M. *et al*. Diffuse γ-ray emission from misaligned active galactic nuclei. *Astrophys. J.* **780,** 161–175 (2014).
24. Ackermann, M. *et al*. GeV observations of star-forming galaxies with the Fermi Large Area Telescope. *Astrophys. J.* **755,** 164–187 (2012).
25. Su, M., Slatyer, T. R. & Finkbeiner, D. P. Giant gamma-ray bubbles from Fermi-LAT: active galactic nucleus activity or bipolar galactic wind? *Astrophys. J.* **724,** 1044–1082 (2010).
26. Crocker, R. M. & Aharonian, F. Fermi bubbles: giant, multibillion-year-old reservoirs of Galactic center cosmic rays. *Phys. Rev. Lett.* **106,** 101102 (2011).
27. Crocker, R. M. *et al*. A unified model of the Fermi Bubbles, microwave haze, and polarized radio lobes: reverse shocks in the Galactic center's giant outflows. *Astrophys. J.* **808,** 107–136 (2015).
28. Cillis, A. N., Hartman, R. C. & Bertsch, D. L. Stacking searches for gamma-ray emission above 100 MeV from radio and Seyfert galaxies. *Astrophys. J.* **601,** 142–150 (2004).

Acknowledgements

We thank D. Finkbeiner, J. Guillochon and L. Sironi for helpful comments on the manuscript. We thank J. Grindlay, V. Kashyap, M. Reid, A. Siemiginowska and S. Portillo for useful discussion. This work is supported by NSF grant AST-1312034.

Author contributions

X.W. and A.L. designed the research. X.W. performed the related calculation and analysed the data. X.W. and A.L. discussed and wrote the manuscript.

Additional information

Supplementary information is available in the online version of the paper. Reprints and permissions information is available online at www.nature.com/reprints. Correspondence and requests for materials should be addressed to X.W.

Competing financial interests

The authors declare no competing financial interests.

Methods

Hydrodynamics of quasar-driven outflows. Outflows are injected into the ambient medium with an initial velocity of $\sim 0.1c$. As they propagate in the ambient medium, a double shock structure forms. The outer forward shock accelerates the swept-up medium, while the inner reverse shock decelerates the wind itself. The equations describing outflow hydrodynamics are given by[17,29]:

$$\frac{\mathrm{d}^2 R_\mathrm{s}}{\mathrm{d}t^2} = \frac{4\pi R_\mathrm{s}^2}{M_\mathrm{s}}(P_\mathrm{T} - P_0) - \frac{GM_\mathrm{tot}}{R_\mathrm{s}^2} - \frac{v_\mathrm{s}}{M_\mathrm{s}}\frac{\mathrm{d}M_\mathrm{s}}{\mathrm{d}t} \tag{2}$$

$$\frac{\mathrm{d}M_\mathrm{s}}{\mathrm{d}t} = 4\pi\rho_\mathrm{g} R_\mathrm{s}^2 v_\mathrm{s} \tag{3}$$

$$\frac{\mathrm{d}P_\mathrm{T}}{\mathrm{d}t} = \frac{\Lambda}{2\pi R_\mathrm{s}^3} - 5P_\mathrm{T}\frac{v_\mathrm{s}}{R_\mathrm{s}} \tag{4}$$

$$\Lambda = L_\mathrm{in} - L_\mathrm{ff} - L_\mathrm{IC} - L_\mathrm{syn} - L_\mathrm{p} \tag{5}$$

where M_s is the swept-up mass of the outflowing shell. M_tot is the gravitational mass decelerating the expansion of the shell, including the mass of dark matter, host galaxy, central black hole (BH) and the self gravity of the shell. The thermal pressure in the shocked wind, P_T, declines at a rate determined by the work done on the medium and radiative losses in the shocked wind, described by the heating/cooling luminosity Λ, composed of energy injection L_in, free–free emission L_ff, synchrotron cooling L_syn, inverse Compton scattering L_IC and proton cooling L_p. Hydrostatic equilibrium gives the thermal pressure in the ambient medium P_0. We assume that quasars radiate at Eddington luminosity $L_\mathrm{Edd} \approx 1.3\times10^{38}(M_\bullet/M_\odot)\,\mathrm{erg\,s^{-1}}$, providing BH mass $M_\bullet$ for a given L_bol. The prescription for assigning $M_\bullet$ to host halo mass M_halo follows Guillochon and Loeb[30], with a fixed bulge to total stellar mass ratio of 0.3. We set an upper limit of M_halo to be $\sim 10^{13} M_\odot$, which is the maximum halo mass that allows the propagation of outflows to halo scale as found in numerical results[17]. We make the assumption of spherical symmetry for the density distribution of the surrounding gas and the mass profile of the galaxy where the outflows are embedded. The gas density distribution is assumed to be a broken power law, expressed as:

$$\rho_\mathrm{g}(R) \propto \begin{cases} R^{-\alpha} & (R < R_\mathrm{disk}) \\ R^{-\beta} & (R_\mathrm{disk} < R < R_\mathrm{vir}) \end{cases} \tag{6}$$

where α and β are different indices for the disk and halo components, and R_disk and R_vir are the radius of the disk and halo, respectively. We fix $\alpha = 2$, assuming an isothermal sphere for the gas within the disk component and β can be self-consistently constrained by halo mass M_halo, redshift z and disk baryonic fraction f_d (taken to be 0.5 in the calculation).

γ-ray spectrum from quasar-driven outflows. We compute the spectral energy distribution (SED) of gamma-ray emission produced by neutral pion (π^0) decay. For $E_\mathrm{p} \lesssim 0.1$ TeV, the γ-ray luminosity is given by[31]:

$$L(E_\gamma) = 2VE_\gamma^2 \int_{E_\mathrm{min}}^{\infty} \frac{q_\pi(E_\pi)}{\sqrt{E_\pi^2 - m_\pi^2 c^4}}\,\mathrm{d}E_\pi \tag{7}$$

where $E_\mathrm{min} = E_\gamma + m_\pi^2 c^4/4E_\gamma$, m_π and E_π are the mass and energy of π^0, and V is the volume of the outflow. $q_\pi(E_\pi)$ is the emissivity of π^0, given by[31]:

$$q_\pi(E_\pi) = \frac{cn_\mathrm{g}}{\kappa_\mathrm{pp}}\sigma_\mathrm{pp}(x)N(x) \tag{8}$$

where $x = m_\mathrm{p}c^2 + E_\pi/\kappa_\mathrm{pp}$, $\kappa_\mathrm{pp} \sim 17\%$ is the fraction of the relativistic proton energy that goes to neutral pions in each interaction, $N(x)$ is the energy distribution of accelerated protons, and $n_\mathrm{g} = \rho_\mathrm{g}/m_\mathrm{p}$ is the number density of the ambient medium. The inelastic cross section of pp collision σ_pp is approximated by[31]:

$$\sigma_\mathrm{pp}(E_\mathrm{p}) \approx 30\,[0.95 + 0.06\ln(E_\mathrm{kin}/\mathrm{GeV})]\,\mathrm{mb} \tag{9}$$

for $E_\mathrm{kin} \geq 1$ GeV, and $\sigma_\mathrm{pp} = 0$ is assumed at lower energies, where $E_\mathrm{kin} = E_\mathrm{p} - m_\mathrm{p}c^2$ is the kinetic energy of protons. This implies that the γ-ray emission is produced by relativistic protons with energy $\gtrsim 2$ GeV. We have verified that the variation in results adopting other approximations of σ_pp is negligible[32]. We estimate that the timescale of Coulomb collisions[33] is ~ 10 times longer than t_pp, meaning that pp collisions are the dominant proton cooling process. The γ-ray SED of an individual quasar outflow for different power-law indices of accelerated protons Γ_p is shown in Supplementary Fig. 2. For a quasar with halo mass $\sim 10^{12} M_\odot$ at redshift $z \sim 0.1$, the expected GeV γ-ray luminosity is $\sim 10^{39}$–$10^{40}\,\mathrm{erg\,s^{-1}}$, which falls off the detection limit of Fermi-LAT by $\sim$2–3 orders of magnitude.

Integrated γ-ray background. The bolometric luminosity function of quasars is given by[18]:

$$\Phi(L_\mathrm{bol}, z) = \frac{\Phi_\star}{(L_\mathrm{bol}/L_\star)^{\gamma_1} + (L_\mathrm{bol}/L_\star)^{\gamma_2}} \tag{10}$$

where L_bol is the bolometric luminosity, $L_\star$ varies with redshift, described by $\log L_\star = (\log L_\star)_0 + k_{L,1}\xi + k_{L,2}\xi^2 + k_{L,3}\xi^3$, $\xi = \log[(1+z)/(1+z_\mathrm{ref})]$, $z_\mathrm{ref} = 2$ and $k_{L,1}$, $k_{L,2}$ and $k_{L,3}$ are free parameters. We adopt parameter values of the pure luminosity evolution model, where $\log(\Phi_\star/\mathrm{Mpc^{-3}}) = -4.733$, $(\log(L_\star/L_\odot))_0 = 12.965$, $L_\odot = 3.9\times10^{33}\,\mathrm{erg\,s^{-1}}$, $k_{L,1} = 0.749$, $k_{L,2} = -8.03$, $k_{L,3} = -4.40$, $\gamma_1 = 0.517$ and $\gamma_2 = 2.096$. We integrate the γ-ray emission over the bolometric luminosity range 10^{42}–$10^{48}\,\mathrm{erg\,s^{-1}}$ and redshift range 0–5. The comoving volume per unit redshift is given by[34]:

$$\frac{\mathrm{d}V}{\mathrm{d}z\,\mathrm{d}\Omega} = D_\mathrm{H}\frac{D_\mathrm{L}^2(z)}{(1+z)^2 E(z)} \tag{11}$$

where $D_\mathrm{H} = c/H_0$ and $E(z) = \sqrt{\Omega_\mathrm{M}(1+z)^3 + \Omega_\Lambda}$. We adopt $H_0 = 70\,\mathrm{km\,s^{-1}\,Mpc^{-1}}$, $\Omega_\mathrm{M} = 0.30$ and $\Omega_\Lambda = 0.7$.

Constraints on radio galaxies' contribution to the EGB. We estimate the contribution to the EGB by radio galaxies (RGs) using samples identified in the most recent Fermi-LAT catalogue, 3FGL[21]. Compared with previous Fermi-LAT catalogues, PKS 0943-76 has been removed due to misassociation[21]. The association of Fornax A (NGC 1316) has not been confirmed by 3FGL[21]. Newly identified FRI (Fanaroff–Riley type I) sources include 4C+39.12 and 3C 264, and FRII sources include 3C 303, 3C 286 and 3C 275.1. Consequently, 19 objects constitute our RG sample; their parameters are summarized in Supplementary Table 1. We note that some FRI sources such as IC 310, PKS 0625-35 and NGC 1275 show blazar-like variabilities, which could lead to debatable source classification with BL Lac objects. TXS 0348+013, 3C 207, 3C 275.1, 3C 286 and 3C 380 are classified as steep-spectrum radio quasars (SSRQs) and thus are non-standard FRIIs[23]. However, FRI/BLL and SSRQ sources are also included in the sample selection of Inoue[22] and Di Mauro and colleagues[23]. Therefore, we keep them in our source selection, to be consistent with previous analysis, and we have verified that their removal leads to negligible changes in radio–γ-ray correlation, as discussed later.

Previously, the contribution of RGs to the EGB has been evaluated based on the γ-ray luminosity function of RGs, which is established from a correlation between γ-ray and 5 GHz 'core-only' radio luminosities of RGs[22]. However, the origin of the γ-ray emission from RGs remains uncertain. γ-ray emission could be produced by ultrarelativistic electrons of high density in the radio lobes by scattering soft photons via self-synchrotron Compton or external Compton processes. Such γ-ray emission has been resolved and confirmed in the lobes of a nearby FRI RG, Cen A, by Fermi-LAT[35]. Due to the lack of simultaneous radio and γ-ray observations of RGs, core variabilities could invalidate this correlation. In our calculation below, we choose radio data closest in date to γ-ray observations. The correlation between the 'core-only' radio luminosity and the total γ-ray luminosity would be distorted if some of the unresolved γ-ray emission originates outside the core of the corresponding galaxies. In such a case, the γ-ray emission from the core would be overestimated, and the radio–γ-ray correlation would provide an upper limit on the contribution of RGs to the EGB. The actual contribution would be between this upper limit and the result one gets when correlating the total radio and γ-ray emission of these galaxies.

We recalculate the L_γ–L_rad correlation for both 'core-only' and total radio luminosity cases using the most recent samples. We follow the BCES (bivariate correlated errors and intrinsic scatter) method by Akritas and Bershady[36] to fit regression parameters and uncertainties. Using the BCES($L_\gamma \mid L_\mathrm{rad}$) slope estimator, we find that the best fit L_γ–$L_\mathrm{rad}^\mathrm{tot}$ and F_γ–$F_\mathrm{rad}^\mathrm{tot}$ correlation can be expressed as:

$$\log(L_{\gamma,40}) = (0.972 \pm 0.087)\log(L_{\mathrm{rad},40}^\mathrm{tot}) + (1.944 \pm 0.233) \tag{12}$$

$$\log(F_\gamma) = (0.682 \pm 0.185)\log(F_\mathrm{rad}^\mathrm{tot}) + (-11.330 \pm 0.141) \tag{13}$$

where $L_{\gamma,40}$ and $L_{\mathrm{rad},40}^\mathrm{tot}$ are L_γ and total radio luminosity $L_\mathrm{rad}^\mathrm{tot}$ in units of $10^{40}\,\mathrm{erg\,s^{-1}}$. Similarly, the best fit L_γ–$L_\mathrm{rad}^\mathrm{core}$ and F_γ–$F_\mathrm{rad}^\mathrm{core}$ are given by:

$$\log(L_{\gamma,40}) = (0.934 \pm 0.073)\log(L_{\mathrm{rad},40}^\mathrm{core}) + (2.582 \pm 0.103) \tag{14}$$

$$\log(F_\gamma) = (0.790 \pm 0.183)\log(F_\mathrm{rad}^\mathrm{core}) + (-10.910 \pm 0.106) \tag{15}$$

where $L_\mathrm{rad}^\mathrm{core}$ is the core-only radio luminosity in units of $10^{40}\,\mathrm{erg\,s^{-1}}$. γ-ray–radio correlations based on 1FGL[22] and 2FGL[23] samples are given by:

$$\log(L_{\gamma,40}) = (1.16 \pm 0.02)\log(L_{\mathrm{rad},40}^\mathrm{core}) + (2.5 \pm 1.41) \tag{16}$$

$$\log(L_{\gamma,40}) = (1.008 \pm 0.025)\log(L_{\mathrm{rad},40}^\mathrm{core}) + (2.32 \pm 1.98) \tag{17}$$

We compare our fitted L_γ–$L_{\rm rad}^{\rm tot}$ and L_γ–$L_{\rm rad}^{\rm core}$ correlation with previous results, shown in Supplementary Figs 3 and 4, respectively. We calculate the corresponding Spearman coefficients and partial correlation coefficient of L_γ and $L_{\rm rad}$, F_γ and $F_{\rm rad}$, and the corresponding p-values, summarized in Supplementary Table 2.

Following Inoue[22] and Di Mauro *et al.*[23], we calculate the contribution of RGs to the EGB using our updated γ-ray–radio correlation. The γ-ray luminosity function (GLF) can be obtained by:

$$\rho_\gamma = \kappa \rho_{\rm rad} \frac{{\rm d}\log L_{\rm rad}}{{\rm d}\log L_\gamma} \tag{18}$$

where $\rho_{\rm rad}$ is the radio luminosity function (RLF) of the RGs, and κ is the fraction of γ-ray loud RGs, constrained by source-count distribution, as discussed later in the text. For the total-radio–γ-ray luminosity correlation, we adopt the total RLF and corresponding parameters given by model C of Willott *et al.*[37] and convert it to the cosmological constants in this work. For the 'core-only' radio luminosity correlation, we convert the total RLF to core RLF, following the method proposed by Di Mauro *et al.*[23], according to the core–total radio luminosity correlation of RGs[38]:

$$\log L_{\rm rad,core}^{\rm 5\,GHz} = (0.77 \pm 0.08) \log L_{\rm rad,tot}^{\rm 1.4\,GHz} + (4.2 \pm 2.1) \tag{19}$$

where core radio luminosity at 5 GHz $L_{\rm rad,core}^{\rm 5\,GHz}$ and total radio luminosity at 1.4 GHz $L_{\rm rad,tot}^{\rm 1.4\,GHz}$ are in units of W Hz^{-1}. We adopt a radio spectral index $\alpha_{\rm r} = 0.8$ for conversion of radio luminosities at different frequencies in our calculation[37].

The intrinsic γ-ray photon flux per unit energy is obtained by:

$$\frac{{\rm d}S_\gamma}{{\rm d}E_\gamma}(E_\gamma, L_\gamma, z, \Gamma) = \frac{2-\Gamma}{E_1^2}\left(\frac{E_\gamma}{E_1}\right)^{-\Gamma}\left[\left(\frac{E_2}{E_1}\right)^{2-\Gamma} - 1\right]^{-1} \times \frac{L_\gamma (1+z)^{2-\Gamma}}{4\pi D_{\rm L}^2(z)} \tag{20}$$

where Γ is the γ-ray photon index. Therefore, we obtain the integrated γ-ray SED from RGs, expressed as:

$$I(E_\gamma) = E_\gamma^2 \int_{\Gamma_{\rm min}}^{\Gamma_{\rm max}} \frac{{\rm d}N_\Gamma}{{\rm d}\Gamma}\,{\rm d}\Gamma \int_{z_{\rm min}}^{z_{\rm max}} \frac{{\rm d}V}{{\rm d}z\,{\rm d}\Omega}\,{\rm d}z \times \int_{L_{\gamma,\rm min}}^{L_{\gamma,\rm max}} {\rm d}\log L_\gamma\, \rho_\gamma(L_\gamma, z) \times \frac{{\rm d}S_\gamma}{{\rm d}E_\gamma}(E_\gamma', z, L_\gamma, \Gamma) \exp[-\tau_{\gamma\gamma}(E_\gamma', z)]\{1 - \omega[S_\gamma(L_\gamma, z)]\} \tag{21}$$

where ${\rm d}N_\Gamma/{\rm d}\Gamma$ is the distribution of γ-ray photon index Γ, which is assumed to be Gaussian, in an analogy to blazars, with an average value of 2.25 and a scatter of 0.28, based on our RG sample. $\omega(S_\gamma)$ is the detection efficiency of Fermi-LAT at a photon flux of S_γ. However, $\omega(S_\gamma)$ is not given in 3FGL, so we adopt the derived detection efficiency for detection threshold TS > 25 and $|b| < 10^\circ$ derived for 2FGL[23]. We adopt $\Gamma_{\rm min} = 1.0$, $\Gamma_{\rm max} = 5.0$, $z_{\rm min} = 0.0$, $z_{\rm max} = 5.0$, $L_{\gamma,\rm min} = 10^{38}$ erg s^{-1} and $L_{\gamma,\rm max} = 10^{50}$ erg s^{-1} in our calculation.

The expected cumulative flux distribution can be obtained by:

$$N_{\rm exp}(>S_\gamma) = 4\pi \int_{\Gamma_{\rm min}}^{\Gamma_{\rm max}} \frac{{\rm d}N_\Gamma}{{\rm d}\Gamma}\,{\rm d}\Gamma \int_{z_{\rm min}}^{z_{\rm max}} \frac{{\rm d}V}{{\rm d}z\,{\rm d}\Omega}\,{\rm d}z \times \int_{L_\gamma(S_\gamma, z)}^{L_{\gamma,\rm max}} \rho_\gamma(L_\gamma, z)\,{\rm d}\log L_\gamma \tag{22}$$

where S_γ is the photon flux above 0.1 GeV and $L_\gamma(S_\gamma, z)$ is the corresponding γ-ray luminosity at a redshift of z. The observed source-count distribution of our sample is given by[39]:

$$N_{\rm obs}(>S_\gamma) = \sum_{i=1}^{N(>S_{\gamma,l})} \frac{1}{\omega(S_{\gamma,i})} \tag{23}$$

where we sum up all RG sources with photon flux $S_{\gamma,i} > S_\gamma$. κ can be constrained by normalizing $N_{\rm exp}$ to $N_{\rm obs}$. We find the best fit at 1σ significance is $\kappa = 0.081 \pm 0.008$ by using total-radio–γ-ray luminosity correlation (equations (12) and (13)), and $\kappa = 2.32 \pm 0.15$ by using core-radio–γ-ray luminosity correlation (equations (14), (15) and (19)). This indicates that the core-only radio–γ-ray correlation overproduces γ-ray loud RGs constraint by the observed source-count distribution. In this case, we fix $\kappa = 1$ in our calculation, following Di Mauro and colleagues[23].

We obtain the resulting integrated γ-ray spectrum for both cases, which set the upper and lower limits of contribution of RGs to the EGB. In our calculation, we adopt the mid-value of this range as the contribution of RGs and show the full range as uncertainty.

We find that the RGs make up $\sim 7 \pm 4\%$ of the EGB. We have verified that if RGs accounts for the rest of the EGB besides blazars and star-forming galaxies at $E_\gamma \lesssim 10$ GeV, then the EGB would be overproduced at higher energies. However, quasar outflow's SED has a generic break at <10 GeV, which naturally accounts for the missing component of the EGB. We note that although our model explains the data, it may not be the only contributor to the missing γ-ray sources, due to uncertainties in its input parameters.

Data availability. The data that support the plots within this paper and other findings of this study are available from the corresponding author upon reasonable request.

References

29. Faucher-Giguère, C.-A. & Quataert, E. The physics of galactic winds driven by active galactic nuclei. *Mon. Not. R. Astron. Soc.* **425,** 605–622 (2012).
30. Guillochon, J. & Loeb, A. The fastest unbound stars in the Universe. *Astrophys. J.* **806,** 124–145 (2015).
31. Aharonian, F. A. & Atoyan, A. M. Broad-band diffuse gamma ray emission of the galactic disk. *Astron. Astrophys.* **362,** 937–952 (2000).
32. Kelner, S. R., Aharonian, F. A. & Bugayov, V. V. Energy specra of gamma rays, electrons, and neutrinos produced at proton–proton interactions in the very high energy regime. *Phys. Rev. D* **74,** 034018 (2006).
33. Sturner, S. J. *et al*. Temporal evolution of nonthermal spectra from supernova remnants. *Astrophys. J.* **490,** 619–632 (1997).
34. Carroll, S. M., Press, W. H. & Turner, E. L. The cosmological constant. *Annu. Rev. Astron. Astrophys.* **30,** 99–542 (1992).
35. Abdo, A. A. *et al*. Fermi gamma-ray imaging of a radio galaxy. *Science* **328,** 725–729 (2010).
36. Akritas, M. G. & Bershady, M. A. Linear regression for astronomical data with measurement errors and intrinsic scatter. *Astrophys. J.* **470,** 706–714 (1996).
37. Willott, C. J. *et al*. The radio luminosity function from the low-frequency 3CRR, 6CE and 7CRS complete samples. *Mon. Not. R. Astron. Soc.* **322,** 536–552 (2001).
38. Lara, L. *et al*. A new sample of large angular size radio galaxies. III. Statistics and evolution of the grown popluation. *Astron. Astrophys.* **421,** 899–911 (2004).
39. Abdo, A. A. *et al*. The first catalog of active galactic nuclei detected by the Fermi Large Area Telescope. *Astrophys. J.* **715,** 429–457 (2010).